**Supporting Information**

# Manipulating Fluorescence of the Exciton-Plasmon Hybrids in the Strong Coupling Regime with Dual Resonance Enhancements

*Yun-Hang Qiu,*[†] *Si-Jing Ding,*[†,‡] *Fan Nan,*[†,ǁ] *Qiang Wang,*[†] *Kai Chen,*[†] *Zhong-Hua Hao,*[†] *Li Zhou,*[†] *Xiaoguang Li,**[,§] *and Qu-Quan Wang**[,†]

[†]Key Laboratory of Artificial Micro- and Nano-structures of the Ministry of Education, Department of Physics, Institute for Advanced Study, Wuhan University, Wuhan 430072, P. R. China

[‡]School of Mathematics and Physics, China University of Geosciences, Wuhan 430074, P. R. China.

[ǁ]Department of Chemical and Biomolecular Engineering, Clarkson University, Potsdam, New York 13699, United States

[§]Institute for Advanced Study, Shenzhen University, Shenzhen 518060, P. R. China

*Email: qqwang@whu.edu.cn; xgli@szu.edu.cn

## 1. Experimental data

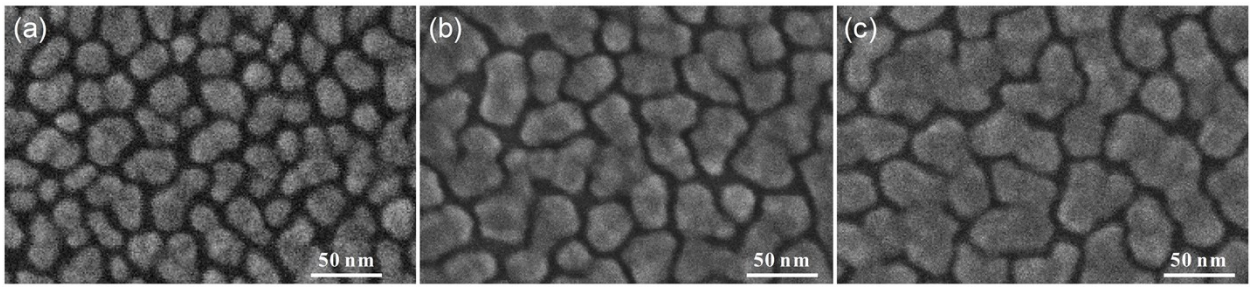


**Fig. S1** SEM images of pure Ag nanoparticle films with varied normalized deposition time $t_d/t_c$ of (a) 0.47, (b) 0.63 and (c) 0.79 with the average particle sizes of 21 nm, 39 nm and 50 nm, respectively. The nanoparticle size increases and the gap decreases with the varied normalized deposition time as the Ag nanoparticle films getting close to semi-continuous percolating films.

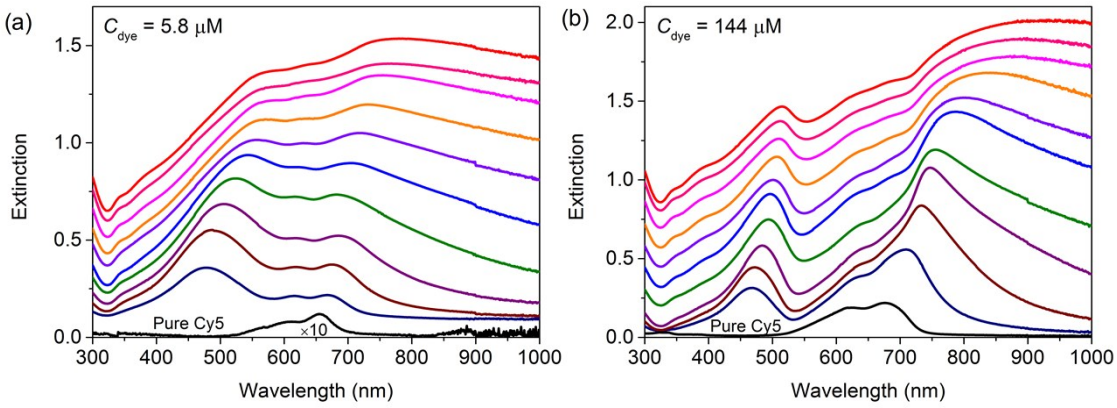


**Fig. S2** Complete extinction spectra of Cy5@Ag hybrids with tunable plasmon resonances and fixed molecular concentrations of (a) 5.8 μM and (b) 144 μM. The bottom spectrum (black line) is the extinction of pure Cy5 molecules on a quartz substrate. The curves have been shifted vertically for clearer presentation.

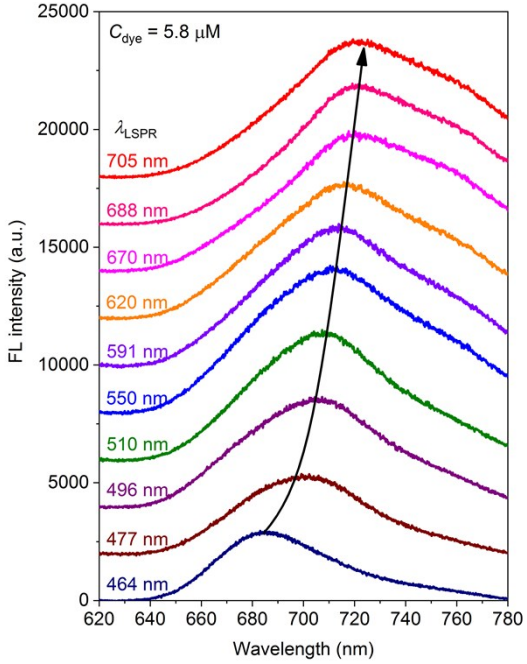


**Fig. S3** Down-conversion fluorescence of Cy5@Ag hybrids with tunable plasmon resonances under the excitation wavelength of 420 nm. The LSPR wavelength of pure Ag film is tuned from 464 nm to 705 nm, and the molecular concentration is fixed at 5.8 μM.

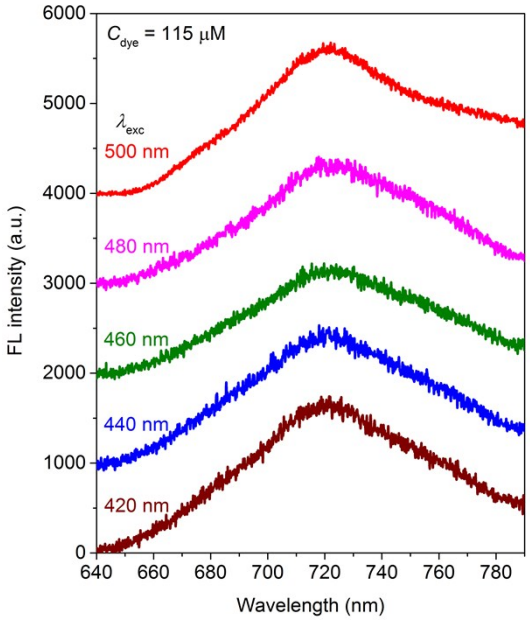


**Fig. S4** Fluorescence spectra of pure Cy5 molecules with fixed molecular concentration of 115 μM under the excitation wavelength from 420 nm to 500 nm.

## 2. Calculations of Rabi splitting with a three-coupled-oscillator model

We use a simplified three-coupled-oscillator model to calculate the Rabi splitting energy[1-3]. A physical system with Hamiltonian $H_0$ is considered. The eigenstates are $|p>$, $|m>$, and $|d>$ with eigenvalues $E_p$, $E_m$, and $E_d$ being associated with the LSPR of Ag nanoparticle films and the Cy5 molecular monomer and dimer excitons, respectively. The coupling Hamiltonian $H$, for which the eigenvalues correspond to the three hybridized resonant peaks can be rewritten as[1]

$$H = \begin{pmatrix} E_p^{'} & V_m & V_d \\ V_m & E_m^{'} & 0 \\ V_d & 0 & E_d^{'} \end{pmatrix}, \tag{S1}$$

where $E_p^{'}$, $E_m^{'}$ and $E_d^{'}$ are the uncoupled eigenvalues modified by changes of the environment. $V_m$ and $V_d$ are the coupling coefficients of LSPR eigenstate and molecular monomer and dimer eigenstates. The Rabi splitting (2Δ) of the Cy5@Ag hybrid system thereby can be written as $2\Delta = V_m + V_d$. For the molecular excitonic states $E_m^{'}$ and $E_d^{'}$, the change in energy only depends on the geometry of the interface rather than the properties of the Ag nanoparticles. Therefore, we have taken $E_m^{'}$ and $E_d^{'}$ directly from the two absorption peaks of the Cy5 dye, $E_m^{'} = E_m$ and $E_d^{'} = E_d$. As we know, $E_p^{'}$ will be modified after introducing the Cy5 dye molecules onto the Ag nanoparticle films, which is quite complicated and hard to determine. To theoretically fit the asymmetric anticross dispersion spectra and find the Rabi splitting energies of the hybrid system, the eigenvalues for Equation (S1) should be calculated. Here we assume that the coupling strength $V_d$ or Rabi splitting 2Δ is a function of bare LSPR wavelength $\lambda_{LSPR}$. For each $\lambda_{LSPR}$, we use the measured UB and LB energies as two of the three eigenvalues of $H$, and the Rabi splitting 2Δ can be determined. Then we obtain the $\lambda_{LSPR}$-dependent Rabi splitting 2Δ shown in Figure 2c. The calculated dispersion curves of the three hybridized resonant bands are obtained and agree well with the experimental data, as seen in the red, black, and blue solid curves in Figure 2a.

## 3. Theoretical Model for Absorption and Emission Spectra of the Hybrid System

### 3.1. Absorption of the hybrid system

The analysis of the absorption behaviours of the hybrid system is based on the linear response theory introduced in our previous study[4]. We first consider the plasmon and exciton equivalently as the electron-hole pairs to construct the non-interacting response function $\chi^0$ of the hybrid system, and then evaluate the interacting response function $\chi$ by using the Dyson equation and considering the interaction between the plasmon and exciton due to the excitation. This approach is in analogy with the earlier linear response theory studies by using the first-principles local density approximation[5-7]. Here, we extend the previous one-plasmon-one-exciton model to the one-plasmon-two-exciton model as follows[4].

We consider the following non-interacting response function

$$\chi^0 = \begin{pmatrix} \dfrac{n_p}{\omega - \omega_p^-} & 0 & 0 \\ 0 & \dfrac{n_d}{\omega - \omega_d^-} & 0 \\ 0 & 0 & \dfrac{n_m}{\omega - \omega_m^-} \end{pmatrix}, \tag{S2}$$

where the subscripts $p$, $d$, and $m$ stands for the plasmon, dipole exciton, and monopole exciton, respectively; $n_i$ indicates the density of the state; The complex frequency $\omega_i^- = \omega_i - i\Gamma_i/2$ gives the frequency and linewidth of the corresponding state; The interaction between the plasmon and two different excitons can be written as

$$K = \begin{pmatrix} 0 & V_{pd}^* & V_{pm}^* \\ V_{pd} & 0 & 0 \\ V_{pm} & 0 & 0 \end{pmatrix}, \tag{S3}$$

and then the plasmon-exciton interacting response function can be obtained from the Dyson equation

$$\chi = \frac{\chi^0}{1 - \chi^0 K}. \tag{S4}$$

The result can be written as

$$\chi = \begin{pmatrix} \chi_{pp} & \chi_{pd} & \chi_{pm} \\ \chi_{dp} & \chi_{dd} & \chi_{dm} \\ \chi_{mp} & \chi_{md} & \chi_{mm} \end{pmatrix}, \tag{S5}$$

where the function $\chi_{ij}$ indicates the response of state $i$ to the excitation on the state $j$. For example, $\chi_{dp}$ indicates the response of the dipole exciton to the field added on the plasmon. The induced charge density relies on the external field

$$V_{\text{ext}} = \begin{pmatrix} V_p \\ V_d \\ V_m \end{pmatrix} \tag{S6}$$

as

$$\rho_{\text{ind}} = \begin{pmatrix} \rho_p \\ \rho_d \\ \rho_m \end{pmatrix} = \chi V_{\text{ext}} \tag{S7}$$

and

$$\rho_i = \sum_j \chi_{ij} V_j , \tag{S8}$$

where $V_i$ indicates the coupling between the state $i$ and external field, and $\rho_i$ is the induced charge oscillation on state $i$. The absorption of the system can be further evaluated from

$$\sigma = \text{Im}(V_{\text{ext}}^* \rho_{\text{ind}}) = \text{Im}(V_{\text{ext}}^* \chi V_{\text{ext}}) = \sum_{ij} \sigma_{ij} \tag{S9}$$

where

$$\sigma_{ij} = \mathrm{Im}(V_i^* \chi_{ij} V_j) \tag{S10}$$

indicates the absorption due to the oscillation of state *i* excited by the field added on the state *j*.

The Cy5 molecule used in this study exhibits two clear absorption modes around 618 nm and 678 nm at high molecular density ($C_{\mathrm{dye}}$ > 50 μM), corresponding to the dipole and monopole excitons, respectively. The two absorption peaks are red-shifted to these values from around 600 nm and 655 nm at very low molecular density.

The coupling strength between excitons and external field can be extracted from the extinction results, where the single exciton extinction decreases as the intensity increasing. This is consistent with the analysis for the peak shifting, namely, the decrease of the extinction for single exciton is due to the spectral weight shifted to the high-energy mode around 300 nm. The extinctions $\alpha$ is determined by the coupling strength $\alpha$ and linewidth $\Gamma$ of the absorption resonance as

$$\alpha = \frac{V^2}{\Gamma}. \tag{S11}$$

So, the coupling between plasmon and external field and energy of the plasmon is extracted from the bare plasmon extinction spectra. In addition, the density of plasmon $n_p$ and exciton $n_c$, where $c=d$ or $m$ for dipole and monopole excitonic modes, respectively, is absorbed into the coupling constant following the relation $V_i \propto \sqrt{n_i}$ and $V_{pi} \propto \sqrt{n_p n_i}$. We evaluate the coupling between plasmon and external field $V_p$ using $V_p = \alpha\Gamma$, where both $\alpha$ and $\Gamma$ are estimated from the experiment. The effective couplings between excitons and external field are $V_d = 0.0076$ eV/μM$^{1/2}$ and $V_m = 0.006$ eV/μM$^{1/2}$, which are estimated by considering absorption spectra at the different molecular concentrations. The effective couplings between plasmon and excitons can be written as $V_{pc} = \sqrt{n_c V_p} V_{pc0}$, where we use $V_{pd0} = 0.03$ (eV/μM)$^{1/2}$ and $V_{pm0} = 0.02$ (eV/μM)$^{1/2}$. In addition, we use $\bar{\omega_d} = (2.01 - i0.13)$ eV and $\bar{\omega_m} = (1.83 - i0.08)$ eV. With these parameters, for example, at

$\omega_p^- = (2.1 - i0.45)$ eV, we have $V_{pd} = 0.28$ eV for the molecular concentration at 115 μM, which satisfies the strong coupling condition $V_{pd} > \frac{\Gamma_p - \Gamma_d}{4}$ for the hybrid system.

With these parameters, we obtain the dispersion of the hybrid system. It tells us that the coupling between plasmon and excitons is roughly a constant for different plasmon mode, and the different Rabi splitting energy is induced by the different mode intensity of the plasmon.

### 3.2. Emission of the hybrid system

To understand the emission behaviour of the hybrid system, we evaluate the total emission intensity as

$$\eta(\lambda_{\text{emi}}) = \sigma_{\text{abs}}(\lambda_{\text{exc}})\sigma_{\text{emi}}(\lambda_{\text{emi}})\sigma_{\text{abs}}(\lambda_{\text{emi}}), \tag{S12}$$

where $\sigma_{\text{abs}}(\lambda)$ and $\sigma_{\text{emi}}(\lambda)$ are the absorption and fluorescence spectra of the hybrid system. It is similar to the previous study[8], that $\sigma_{\text{abs}}(\lambda)$ provides the fluorescence enhancement manifesting the Purcell effect and $\sigma_{\text{emi}}(\lambda)$ is the fluorescence spectrum without the Purcell effect. However, the difference is that we consider $\sigma_{\text{emi}}(\lambda)$ as the fluorescence of the plexciton due to the coherent coupling between plasmon and exciton, and launched by the energy on the molecules.

Since the emission process can be viewed as the time reversal process of the absorption, the spectrum $\sigma_{\text{emi}}(\lambda)$ can be evaluated by using the linear response theory similar as the absorption spectrum $\sigma_{\text{abs}}(\lambda)$ . However, the difference is that some fast dissipation processes should be considered during the emission. One is relaxation of the vibration mode, which gives the Stokes shift of the emission peak. The other is the relaxation of the plasmon mode, which largely suppresses the contribution of the plasmon charge oscillation to the spectrum.

The Stokes shift of the fluorescence is considered by using a different bare molecular absorption peak in the calculation. As shown in the experiment, the absorption peak is around 620 and 680 nm (1.82 eV). In the theoretical study, we assume the fluorescence peak of the bare molecule $\lambda_{\text{emi}}$ is around 725 nm (1.71 eV).

To consider the plasmon relaxation, we start from the excitation of the system with one plasmon and one exciton states. In analogy to the above one-plasmon-two-exciton model, we consider the following non-interacting response function

$$\chi^0 = \begin{pmatrix} \dfrac{n_p}{\omega - \omega_p^-} & 0 \\ 0 & \dfrac{n_e}{\omega - \omega_e^-} \end{pmatrix}, \tag{S13}$$

where the subscripts $p$ and $e$ stands for the plasmon, and emission exciton, respectively. The interaction between the plasmon and two different excitons is written as

$$K = \begin{pmatrix} 0 & V_{pe}^* \\ V_{pe} & 0 \end{pmatrix}, \tag{S14}$$

and the plasmon-exciton interacting response function can be written as

$$\chi = \begin{pmatrix} \chi_{pp} & \chi_{pe} \\ \chi_{ep} & \chi_{ee} \end{pmatrix}. \tag{S15}$$

The induced charge density relies on the external field

$$V_{\text{ext}} = \begin{pmatrix} V_p \\ V_e \end{pmatrix} \tag{S16}$$

as

$$\rho_{\text{ind}} = \begin{pmatrix} \rho_p \\ \rho_e \end{pmatrix} = \chi V_{\text{ext}} \tag{S17}$$

and

$$\rho_i = \sum_j \chi_{ij} V_j \ . \tag{S18}$$

Now, by considering the damping of the plasmon, we realize that the charge oscillation on the metal will be quickly nonradiatively damped due to a much larger linewidth comparing with the molecule. Consequently, the charge oscillation participates in the emission process is dominated by the $\rho_e$, and $\rho_p$ is largely damped. Therefore, to simulate the emission spectrum, we can introduce a damping matrix added on $\rho_{\text{ind}}$ as

$$\rho'_{\text{ind}} = D\rho_{\text{ind}} = \begin{pmatrix} \delta & 0 \\ 0 & 1 \end{pmatrix} \rho_{\text{ind}} = \begin{pmatrix} \delta\rho_p \\ \rho_e \end{pmatrix}, \tag{S19}$$

the damped density $\rho'_{\text{ind}}$ is then used to evaluate the emission spectrum as

$$\sigma_{\text{emi}} = \text{Im}(V^*_{\text{ext}} D\rho_{\text{ind}}) = \text{Im}(V^*_{\text{ext}} D\chi V_{\text{ext}}) = \delta(\sigma_{pp} + \sigma_{pe}) + (\sigma_{ee} + \sigma_{ep}) \ . \tag{S20}$$

In our simulation, we choose $\delta = 0$ for simplicity. For the other parameters, we have $V_{e0} = 0.003$ eV/μM$^{1/2}$, $V_{pe0} = 0.01$ (eV/μM)$^{1/2}$, and $\omega_e^- = (1.71 - i0.08)$ eV.

**References**


(1) Cade, N. I.; Ritman-Meer, T.; Richards, D. *Phys. Rev. B* **2009**, 79, 241404.

(2) Wurtz, G. A.; Evans, P. R.; Hendren, W.; Atkinson, R.; Dickson, W.; Pollard, R. J.; Zayats, A. V.; Harrison, W.; Bower, C. *Nano Lett.* **2007**, *7*, 1297.

(3) Bellessa, J.; Symonds, C.; Meynaud, C.; J. Plenet, C.; Cambril, E.; Miard, A.; Ferlazzo, L.; Lemaître, A. *Phys. Rev. B* **2008**, *78*, 205326.

(4) Ding, S.-J.; Li, X.; Nan, F.; Zhong, Y.-T.; Zhou, L.; Xiao, X.; Wang, Q.-Q.; Zhang, Z. *Phys. Rev. Lett.* **2017**, *119*, 177401.

(5) Li, X.; Xiao, D.; Zhang, Z. *New J. Phys.* **2013**, *15*, 023011.

(6) Ekardt, W. *Phys. Rev. B* **1985**, *31*, 6360.

(7) Zangwill, A. and Soven, P. *Phys. Rev. A* **1980**, *21*, 1561.

(8) Tanaka, K.; Plum, E.; Ou, J. Y.; Uchino, T.; Zheludev, N. I. *Phys. Rev. Lett.* **2010**, *105*, 227403.